

SCANNING ELECTRON MICROSCOPE STUDIES ON AGGREGATION CHARACTERISTICS OF ALUMINA NANOFLUIDS

**INTERIM REPORT
TFLRF No. 443**

by
Nigil S. Jeyashekar, Ph.D., P.E.

**U.S. Army TARDEC Fuels and Lubricants Research Facility
Southwest Research Institute® (SwRI®)
San Antonio, TX**

for
**Bridget L. Dwornick, Allen S. Comfort, and
Dr. James S. Dusenbury
U.S. Army TARDEC
Force Projection Technologies
Warren, Michigan**

Contract No. W56HZV-09-C-0100 (WD17–Task 4)

UNCLASSIFIED: Distribution Statement A. Approved for public release

August 2013

Disclaimers

Reference herein to any specific commercial company, product, process, or service by trade name, trademark, manufacturer, or otherwise, does not necessarily constitute or imply its endorsement, recommendation, or favoring by the United States Government or the Department of the Army (DoA). The opinions of the authors expressed herein do not necessarily state or reflect those of the United States Government or the DoA, and shall not be used for advertising or product endorsement purposes.

Contracted Author

As the author(s) is(are) not a Government employee(s), this document was only reviewed for export controls, and improper Army association or emblem usage considerations. All other legal considerations are the responsibility of the author and his/her/their employer(s).

DTIC Availability Notice

Qualified requestors may obtain copies of this report from the Defense Technical Information Center, Attn: DTIC-OCC, 8725 John J. Kingman Road, Suite 0944, Fort Belvoir, Virginia 22060-6218.

Disposition Instructions

Destroy this report when no longer needed. Do not return it to the originator.

UNCLASSIFIED

SCANNING ELECTRON MICROSCOPE STUDIES ON AGGREGATION CHARACTERISTICS OF ALUMINA NANOFLUIDS

**INTERIM REPORT
TFLRF No. 443**

by
Nigil S. Jeyashekar, Ph.D., P.E.

**U.S. Army TARDEC Fuels and Lubricants Research Facility
Southwest Research Institute® (SwRI®)
San Antonio, TX**

for
**Bridget L. Dwornick, Allen S. Comfort, and
Dr. James S. Dusenbury
U.S. Army TARDEC
Force Projection Technologies
Warren, Michigan**

**Contract No. W56HZV-09-C-0100 (WD17–Task 4)
SwRI® Project No. 08.14734.17.401**

UNCLASSIFIED: Distribution Statement A. Approved for public release

August 2013

Approved by:



**Gary B. Bessee, Director
U.S. Army TARDEC Fuels and Lubricants
Research Facility (SwRI®)**

UNCLASSIFIED

REPORT DOCUMENTATION PAGE				Form Approved OMB No. 0704-0188	
Public reporting burden for this collection of information is estimated to average 1 hour per response, including the time for reviewing instructions, searching existing data sources, gathering and maintaining the data needed, and completing and reviewing this collection of information. Send comments regarding this burden estimate or any other aspect of this collection of information, including suggestions for reducing this burden to Department of Defense, Washington Headquarters Services, Directorate for Information Operations and Reports (0704-0188), 1215 Jefferson Davis Highway, Suite 1204, Arlington, VA 22202-4302. Respondents should be aware that notwithstanding any other provision of law, no person shall be subject to any penalty for failing to comply with a collection of information if it does not display a currently valid OMB control number. PLEASE DO NOT RETURN YOUR FORM TO THE ABOVE ADDRESS.					
1. REPORT DATE (DD-MM-YYYY) 27-08-2013		2. REPORT TYPE Interim Report		3. DATES COVERED (From - To) June 2011 – December 2013	
4. TITLE AND SUBTITLE Scanning Electron Microscope Studies on Aggregation Characteristics of Alumina Nanofluids				5a. CONTRACT NUMBER W56HZV-09-C-0100	
				5b. GRANT NUMBER	
				5c. PROGRAM ELEMENT NUMBER	
6. AUTHOR(S) Jeyashekar, Nigil				5d. PROJECT NUMBER SwRI 08.14734.17.401	
				5e. TASK NUMBER WD 17 (Task 4)	
				5f. WORK UNIT NUMBER	
7. PERFORMING ORGANIZATION NAME(S) AND ADDRESS(ES) U.S. Army TARDEC Fuels and Lubricants Research Facility (SwRI®) Southwest Research Institute® P.O. Drawer 28510 San Antonio, TX 78228-0510				8. PERFORMING ORGANIZATION REPORT NUMBER TFLRF No. 443	
9. SPONSORING / MONITORING AGENCY NAME(S) AND ADDRESS(ES) U.S. Army RDECOM U.S. Army TARDEC Force Projection Technologies Warren, MI 48397-5000				10. SPONSOR/MONITOR'S ACRONYM(S)	
				11. SPONSOR/MONITOR'S REPORT NUMBER(S)	
12. DISTRIBUTION / AVAILABILITY STATEMENT UNCLASSIFIED: Dist A Approved for public release; distribution unlimited					
13. SUPPLEMENTARY NOTES					
14. ABSTRACT This research study establishes the relationship between sonication parameters and overall particle volume fraction in the base fluid, to the volume fraction of nanoparticles in the aggregate cluster and overall thermal conductivity enhancement of the nanofluid. The test matrix includes two power levels, with five overall particle volume fractions at each power level, and five sonication times for each overall particle volume fraction. The research concludes that sonication time has negligible effect on cluster size and number of particles per aggregate cluster at a constant overall particle volume fraction and vice versa. The research also concludes that nanofluid with higher thermal conductivity can be obtained when cluster size is limited to 200 nm. It is recommended that future research should emphasize on particle modification, such as encapsulation, to optimize and achieve an aggregate cluster size limit of 200 nm.					
15. SUBJECT TERMS Aggregates, Clusters, Nanofluid, Nanoparticle, Scanning Electron Microscope, Sonication, Thermal Conductivity					
16. SECURITY CLASSIFICATION OF:			17. LIMITATION OF ABSTRACT	18. NUMBER OF PAGES	19a. NAME OF RESPONSIBLE PERSON NIGIL SATISH JEYASHEKAR
a. REPORT Unclassified	b. ABSTRACT Unclassified	c. THIS PAGE Unclassified	Unclassified	34	19b. TELEPHONE NUMBER (include area code) 210-522-2533

EXECUTIVE SUMMARY

Nanofluids are prepared by dispersing nanoparticles in base fluid using a sonicator for a fixed period of time and at a fixed power level, thereby imparting a specific energy density to the nanofluid. Extensive literature review on thermal conductivity enhancement in nanofluids does not reference a standardized procedure for preparing nanofluids. The time period for sonication and power level varies among peer reviewed literature and its relationship to nanoparticle aggregation characteristics and overall nanofluid thermal conductivity has not been determined. The current research work fills this technical void by determining the effect of sonication time and overall nanoparticle volume fraction on aggregation characteristics of nanoparticles in a base fluid. The two aggregation parameters investigated are cluster size and volume fraction of nanoparticles in a single aggregate cluster. Furthermore, determining the thermal conductivity of the aggregates as a function of cluster size establishes a limit on the maximum size limit on clusters in a nanofluid in order to achieve high thermal conductivity.

The research work is accomplished by obtaining the aforementioned aggregation parameters from a matrix of nanofluid samples containing alumina nanoparticles (40 nm nominal diameter) dispersed in deionized water. The matrix includes two sonication power levels (70 W and 100 W). At each power level, the matrix contains five nanofluid samples with overall volume fractions ranging from 1% to 5%. Five samples are taken at each volume fraction and sonicated for five different sonication times. The sonication times for 70 W ranges from 20 minutes to 80 minutes, whereas for 100 W, the sonication time ranges from 14 minutes to 56 minutes. The test matrix is designed such that the energy density imparted to the nanofluid samples at both power levels are the same. Such a test matrix design enables comparison of the effects of sonication time and overall volume fraction on aggregation characteristics at two different power levels. The nanofluid samples are then placed on a carbon grid for image acquisition using Scanning Electron Microscope (SEM). The resulting image is analyzed using Clemex Vision PE[®] image analysis tool to obtain particle size distribution and fractal dimension. This data is further processed to obtain the number of nanoparticles and volume fraction of nanoparticles in a single aggregate cluster.

The cluster size distribution and the number of particles per cluster in the alumina nanofluid have been characterized as a function of sonication time and overall nanoparticles volume fraction at two different power levels. It has been concluded that at both power levels, sonication time has negligible effect on the cluster size and the number of particles per cluster when the overall volume fraction is a constant and vice versa. The smaller clusters that contain larger fraction of particles compared to the base fluid will have a higher thermal conductivity compared to larger clusters with fewer particles and a large volume fraction of the base fluid. It has been concluded that the overall thermal conductivity enhancement can be maximized by limiting the cluster size to a hydraulic mean diameter less than 200 nm. The thermal conductivity of the clusters are marginally higher than the base fluid and remains almost a constant for all clusters with size greater than 200 nm.

The results from this research has established the fact that optimizing the cluster distribution to yield nanofluids with superior thermal characteristics cannot be solely achieved by sonication parameters, such as time or power level. It is recommended that future work should emphasize on other methods to optimize aggregate cluster size, such as surface modification of nanoparticles by encapsulation, prior to dispersion in the base fluid and hence, study its effect on overall thermal conductivity of the nanofluid.

FOREWORD/ACKNOWLEDGMENTS

The U.S. Army TARDEC Fuel and Lubricants Research Facility (TFLRF) located at Southwest Research Institute (SwRI), San Antonio, Texas, performed this work during the period June 2011 through December 2013 under Contract No. W56HZV-09-C-0100. The U.S. Army Tank Automotive RD&E Center, Force Projection Technologies, Warren, Michigan administered the project. Mr. Eric Sattler (RDTA-SIE-ES-FPT) served as the TARDEC contracting officer's technical representative. Ms. Bridget Dwornick, Mr. Allen Comfort, and Dr. Jay Dusenbury of TARDEC served as project technical monitors.

The authors would like to acknowledge the contribution of the TFLRF technical support staff, the University of Texas at San Antonio along with the administrative and report-processing support provided by Dianna Barrera.

TABLE OF CONTENTS

<u>Section</u>	<u>Page</u>
EXECUTIVE SUMMARY	v
FOREWORD/ACKNOWLEDGMENTS	vii
LIST OF TABLES	ix
LIST OF FIGURES	ix
ACRONYMS AND ABBREVIATIONS	x
1.0 INTRODUCTION AND OBJECTIVE	1
2.0 THEORY: ACOUSTIC CAVITATION AND AGGLOMERATION	2
3.0 PROJECT SCOPE	3
4.0 NANOFLUIDS PREPARATION AND TEST MATRIX	3
5.0 SEM IMAGE ACQUISITION	4
6.0 IMAGE PROCESSING AND DATA EXTRACTION	5
6.1 IMAGE CALIBRATION	6
6.2 IMAGE PROCESSING AND MODIFICATION	6
6.3 DATA EXTRACTION	8
6.4 AGGREGATE SIZE DISTRIBUTION ANALYSIS	8
7.0 RESULTS: ANALYSIS AND INFERENCE	9
8.0 CONCLUSIONS AND RECOMMENDATIONS FOR FUTURE WORK	12
9.0 REFERENCES	13
 APPENDIX A. SEM Images of Alumina Nanofluids at Different Sonication times, Volume Fractions and Sonication Power Levels	 A-1

LIST OF TABLES

<u>Table</u>	<u>Page</u>
Table 1. Alumina Nanofluids Matrix.....	3
Table 2. Test Matrix for SEM Measurements	4

LIST OF FIGURES

<u>Figure</u>	<u>Page</u>
Figure 1. Hitachi S-500 Scanning Electron Microscope Instrument	5
Figure 2. SEM Image of Alumina Nanofluid	6
Figure 3. Intensity Histogram of SEM Image (in Figure 2)	7
Figure 4. SEM Image Modified for Data Extraction	7
Figure 5. Volume Fraction of Nanoparticles in the Aggregate versus Cluster Diameter as a function of sonication time at 70 W	9
Figure 6. Volume Fraction of Nanoparticles in the Aggregate versus Cluster Diameter as a function of Overall Volume Fraction of Alumina Nanoparticles at 70 W	10
Figure 7. Volume Fraction of Nanoparticles in the Aggregate versus Cluster Diameter as a function of sonication time at 100 W	11
Figure 8. Volume Fraction of Nanoparticles in the Aggregate versus Cluster Diameter as a function of Overall Volume Fraction of Alumina Nanoparticles at 100 W	11
Figure 9. Thermal Conductivity of Clusters at 100 W for all Sonication Times and Overall Volume Fraction of Alumina Nanoparticles	12
Figure A-1. $\phi_{\text{overall}} = 1\%$, $P = 70 \text{ W}$	A-2
Figure A-2. $\phi_{\text{overall}} = 2\%$, $P = 70 \text{ W}$	A-3
Figure A-3. $\phi_{\text{overall}} = 3\%$, $P = 70 \text{ W}$	A-4
Figure A-4. $\phi_{\text{overall}} = 4\%$, $P = 70 \text{ W}$	A-5
Figure A-5. $\phi_{\text{overall}} = 5\%$, $P = 70 \text{ W}$	A-6
Figure A-6. $\phi_{\text{overall}} = 1\%$, $P = 100 \text{ W}$	A-7
Figure A-7. $\phi_{\text{overall}} = 2\%$, $P = 100 \text{ W}$	A-8
Figure A-8. $\phi_{\text{overall}} = 3\%$, $P = 100 \text{ W}$	A-9
Figure A-9. $\phi_{\text{overall}} = 4\%$, $P = 100 \text{ W}$	A-10
Figure A-10. $\phi_{\text{overall}} = 5\%$, $P = 100 \text{ W}$	A-11

ACRONYMS AND ABBREVIATIONS

%	Percent
ϕ_{int}	Volume fraction of nanoparticles in a single aggregate cluster
$\phi_{overall}$	Overall volume fraction of nanoparticles in the base fluid
d_f	Fractal dimension
DLS	Dynamic Light Scattering
k_{cl}	Thermal Conductivity of Clusters in the Base Fluid
KJ	Kilo Joule
KV	Kilo Volt
m/s	meter per second
mg	milligram
min	minute
ml	milliliter
nm	nanometer
N_{int}	Number of alumina nanoparticles in a single aggregate cluster
r_{cl}	Radius of the cluster
r_p	Radius of the alumina nanoparticles (20 nm)
SEM	Scanning Electron Microscope
SwRI	Southwest Research Institute
TARDEC	Tank Automotive Research, Development and Engineering Center
TFLRF	U.S. Army TARDEC Fuels and Lubricants Research Facility
UTSA	University of Texas at San Antonio
W	Watts
YAG	Yttrium Aluminum Garnett (<i>Molecular Formula: $Y_3Al_5O_{12}$</i>)

1.0 INTRODUCTION AND OBJECTIVE

Thermal conductivity enhancement of nanofluids have been researched and reviewed through experimental studies and mathematical modeling (Jeyashekar *et al.*, 2012). The current method employed by researchers to prepare such nanofluids involve dispersing nanoparticles in a base coolant followed by sonication for a specified time period at power level. A comprehensive literature review by Özerinç *et al.*, 2009, presents a comparison between thermal conductivity enhancement data among similar nanofluid samples published by various researchers. These peer reviewed papers do not contain a standardized procedure for preparing the nanofluid sample and the method that has been followed by various researchers to prepare these nanofluids varied significantly in terms of sonication time periods and power levels. This implies that the size distribution of aggregate clusters varied significantly among the different peer reviewed publications and the aggregate cluster size distribution, in turn, governs the overall thermal conductivity of the nanofluid (Wang *et al.*, 2003). Therefore the research need is to understand the relationship between sonication parameters, nanoparticles aggregation characteristics and how cluster size affects the overall thermal conductivity of the nanofluid.

In the current project, alumina nanofluid in deionized water is prepared at five volume fractions ranging from 1% to 5%. At each volume fraction, five nanofluid samples will be taken and be subjected to five sonication time periods ranging from 20 minutes to 80 minutes at a constant power level of 70 W. This procedure is repeated with a new batch of nanofluid samples at each volume fraction, with sonication time period ranging from 14 minutes to 56 minutes, at power level of 100 W. For a given volume fraction, the five nanofluid samples, at both power levels, have the same energy densities imparted by sonication. These sonicated samples are imaged using Scanning Electron Microscope (SEM), followed by image processing to obtain size distribution of nanoparticle clusters.

The primary objective of the project is to examine if a predictable relationship exists between volume fraction of nanoparticles per aggregate cluster versus cluster size distribution for different sonication time periods and overall particle volume fractions ranging from 1% to 5%, at two different power levels (70 W and 100 W). These aggregation characteristics will be used to

determine the thermal conductivity of clusters as a function of cluster size. This result will be used to determine the optimum cluster size that should be achieved to maximize the overall thermal conductivity of the nanofluid.

2.0 THEORY: ACOUSTIC CAVITATION AND AGGLOMERATION

The phenomenon of acoustic cavitation refers to the formation, growth and implosive collapse of bubbles in a liquid due to ultrasound that passes through the liquid. In a sonicating bath or ultrasonic homogenizer, the series of compression and expansion waves, exert pressure on the surrounding liquid resulting in acoustic cavitation. The formation of microbubbles is nucleated by the presence of alumina nanoparticles. The ultrasonic waves feed energy to the microbubble causing it to grow during the expansion wave phase and shrink during the compressive wave phase. As microbubbles coalesce, the growth rate is sustained allowing little or no compression. The implosive collapse occurs when the microbubble reaches an unstable size coupled with the fact that the frequency of the expansion-compression cycle of the microbubble is in resonance with the acoustic field of the sonicator. The conditions that produce acoustic cavitation results in the collapse of the microbubble that can generate extreme temperatures and pressures within the void, which is often referred to as the hot spot. The cooler temperatures of the surrounding bulk fluid, quenches the hot spot rapidly. The formation and study of these hot spots is the basis of sonochemistry.

The relating physical effects of ultrasound on nanoparticles agglomeration in the coolant, during sonication, have been discussed extensively in the literature (Oxley, 2003). This work describes specifically the sonochemistry in liquid-solid media. The implosive collapse of the microbubble results in the release of the gas contained within, as a microjet with speeds in excess of 100 m/s, greatly enhancing the mass transport of nanoparticles in the fluid causing interparticle collision. The intensity of the collision provides enough energy to spot weld the two nanoparticles at the point of contact. Research has shown that the degree of agglomeration initiated by cavitation is directly related to the melting point of the particles. When such collisions are direct the volume fraction and number of nanoparticle clusters increases. Further collisions between two or more clusters and nanoparticles causes growth of the aggregated clusters in the nanofluid. As the

cluster mass increases, the velocity decreases causing low intensity collisions between larger clusters and nanoparticles; and therefore the probability of cluster growth decreases. This theory is consistent with experimental results obtained from Dynamic Light Scattering (DLS) studies (Jeyashekar *et al.*, 2012).

3.0 PROJECT SCOPE

The contract for work directive 17 under task 4 requires SwRI to make fifty (50) physical property measurements of nanofluids and conduct research based on those measurements. Based on the aforementioned objectives, alumina nanofluids in deionized water will be prepared at five (50) volume fractions, ranging from 1% to 5%. Five samples from each volume fraction will be subjected to different sonication times. This provides twenty-five (25) unique nanofluid samples for SEM image acquisition. Since the objective of this project includes two power levels, fifty (50) SEM measurements will be obtained and the respective aggregate cluster size distributions are classified under physical property measurements. Therefore, the project objectives fulfill the scope of the proposed contract.

4.0 NANOFLUIDS PREPARATION AND TEST MATRIX

The required mass of alumina nanoparticle powder, with 40 nm nominal diameter, was mixed with 25 ml of deionized water to prepare nanofluid samples at particle volume concentrations ranging from 1% to 5%, as shown in Table 1.

Table 1. Alumina Nanofluids Matrix

Sample ID	Particle volume fraction (%)	Volume of deionized water (ml)	Mass of alumina nanoparticles powder (mg)
Sample-1	1	25	934.3434
Sample-2	2	25	1887.755
Sample-3	3	25	2860.825
Sample-4	4	25	3854.167
Sample-5	5	25	4868.421

The test matrix for obtaining SEM images with nanofluid samples subjected to five (5) sonication time periods at each volume fraction, at each power level is shown in Table 2 along with the respective energy densities.

Table 2. Test Matrix for SEM Measurements

Power (W)	Sonication time				
	t₁ = 20.0 min.	t₂ = 35.0 min.	t₃ = 50.0 min.	t₄ = 65.0 min.	t₅ = 80.0 min.
70 W	Sample-1	Sample-1	Sample-1	Sample-1	Sample-1
	Sample-2	Sample-2	Sample-2	Sample-2	Sample-2
	Sample-3	Sample-3	Sample-3	Sample-3	Sample-3
	Sample-4	Sample-4	Sample-4	Sample-4	Sample-4
	Sample-5	Sample-5	Sample-5	Sample-5	Sample-5
100 W	t₁ = 14.0 min.	t₂ = 24.5 min.	t₃ = 35.0 min.	t₄ = 45.5 min.	t₅ = 56.0 min.
	Sample-1	Sample-1	Sample-1	Sample-1	Sample-1
	Sample-2	Sample-2	Sample-2	Sample-2	Sample-2
	Sample-3	Sample-3	Sample-3	Sample-3	Sample-3
	Sample-4	Sample-4	Sample-4	Sample-4	Sample-4
	Sample-5	Sample-5	Sample-5	Sample-5	Sample-5
Energy Density (KJ/ml)	3.3264	5.7624	8.1480	10.483	12.768

5.0 SEM IMAGE ACQUISITION

Figure 1 shows the Hitachi S-500 SEM instrument at the University of Texas at San Antonio (UTSA), used to acquire images of nanoparticle aggregates to determine size distribution. The nanofluid sample is placed on a carbon film supported with copper grids with a mesh size of 300, prior to SEM image acquisition. SEM measurements are made immediately after sample preparation. The SEM instrument is equipped with detectors in bright field and dark field modes, which register the electrons simultaneously. The SEM microscope has a field-emission gun with a 0.4 nm spatial resolution operated at 30 KV. Spatially resolved chemical analysis by X-ray emission spectroscopy is equipped with a solid-state Bruker, elemental line scanning along with

two dimensional mapping. Qualitative chemical information can be obtained from the topography of a material by using an automated YAG backscattered electron detector. Since, the objective is to obtain morphological information to estimate particle size distribution of the aggregates, the elemental scanning was not incorporated as a part of the measurements.



Figure 1. Hitachi S-500 Scanning Electron Microscope Instrument at UTSA

6.0 IMAGE PROCESSING AND DATA EXTRACTION

Figure 2 shows an SEM image of alumina nanofluid sample at 1% volume fraction sonicated for 20 minutes at a power level of 70 W. The energy density imparted to the nanofluid is 3.353 KJ/ml. Based on the Figure 2, it should be noted that the agglomeration process begins with nanoparticles aggregating as strings as a consequence of acoustic cavitation, followed by growth to become a well rounded cluster of nanoparticles distributed throughout the SEM image. The dark spots on the upper and lower right hand corner of the image is vacuum that results due to sample spreading extremely thin on the carbon film used for SEM image acquisition. The algorithm and subroutine used for image processing and data extraction is described in the following subsections for one SEM image, prior presenting to aggregate size distribution results.

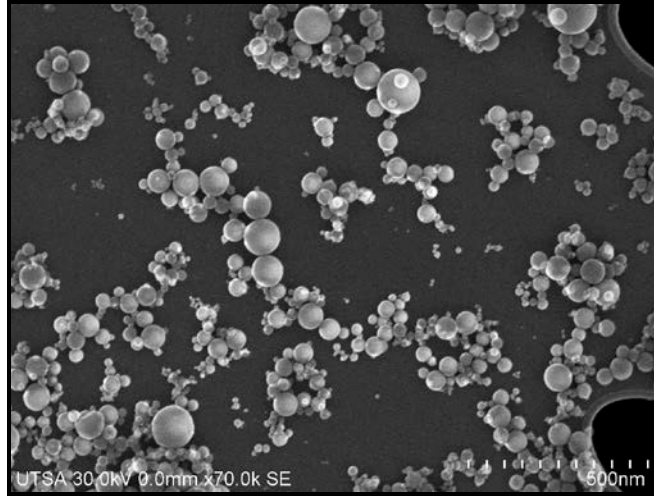


Figure 2. SEM Image of Alumina Nanofluid

6.1 IMAGE CALIBRATION

Figure 2 is a 1280 x 960 pixel image and was acquired at a magnification factor of 70,000 with a scale bar set at 500 nm, shown at the bottom right hand corner of the SEM image. The image calibration process involves converting the SEM image described in term of pixel units to nanometers. The calibration must be done in order to estimate the particle size distribution in nanometer units. In this step, an electronic caliper will be programmed to measure the length of the horizontal scale bar in terms of pixel units. The actual length of this scale bar at 500 nm corresponds to 156.25 pixels. This results in a calibration factor of 1.4205 nm per pixel. Therefore, the nanoparticles aggregates in this image are distributed over an area of 1818.18 nm x 1363.64 nm.

6.2 IMAGE PROCESSING AND MODIFICATION

The actual SEM image in Figure 2 does not have a sharp contrast between the particle and the background and therefore limits data extraction. The purpose of this step is to create a sharp contrast between the nanoparticles and the background, thereby clearly defining the particle boundaries and minimizing the errors made in estimating the aggregate size distribution histogram. A gray image has pixels rated from 0 (black) to 255 (white). A threshold selected between intensities of 79 and 255, selects only nanoparticles in the image for aggregate size

distribution. Figure 3 shows the complete pixel intensity histogram of the SEM image (from Figure 2) and the aggregated particle pixel intensity peaks are shown from 79 to 255. The remaining pixel intensities from 0 to 78 refers to the background.

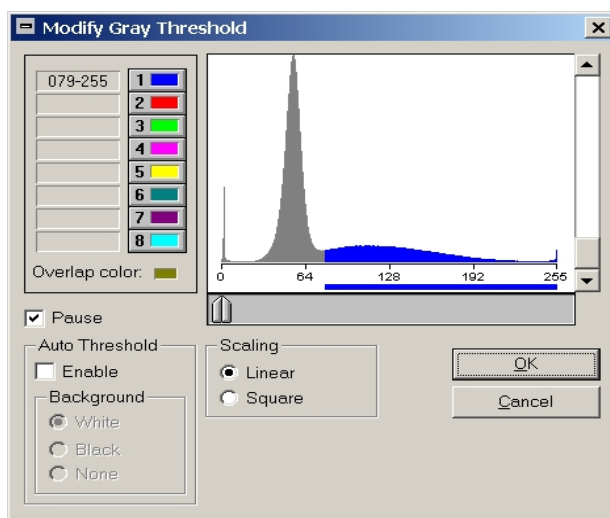


Figure 3. Intensity Histogram of SEM Image (in Figure 2)

Figure 4 shows the processed SEM image with the nanoparticle aggregates that are displayed in blue, which is in contrast to the dark background. This modified SEM image is ready for data extraction.

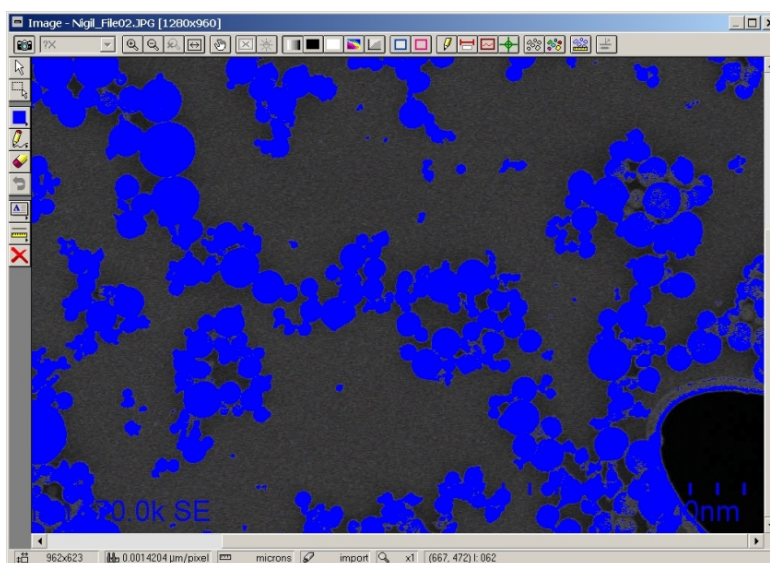


Figure 4. SEM Image Modified for Data Extraction

6.3 DATA EXTRACTION

The data extraction is performed using a code written to process SEM images using Clemex Vision PE[®] image processing tool. The computation is performed by dividing the image area into grids, followed by scanning the entire image to locate the grids shaded in blue in order to estimate the diameter of the particle. This procedure is started with grid dimension corresponding to the smallest particle in the image. The grid size is incremented in steps and the image scan is performed several times until the largest particle in the image (shaded in blue) has been represented. This algorithm estimates the hydraulic mean diameter of the aggregates and provides the fractal dimensions of such aggregates. The subroutine and details on sub-functions of the program code are beyond the scope of this task and are not presented in this report.

6.4 AGGREGATE SIZE DISTRIBUTION ANALYSIS

Each aggregate is a percolating cluster containing aggregates of alumina nanoparticles with base fluid present inside these clusters. If the radius of the percolating cluster is r_{cl} and the radius of the alumina nanoparticle is r_p , then the number of alumina nanoparticles present in a single aggregate is given by equation 1.

$$N_{int} = \left(\frac{r_{cl}}{r_p} \right)^{d_f} \rightarrow (1)$$

The volume fraction of alumina nanoparticles in a single aggregate cluster (ϕ_{int}) is given by equation 2.

$$\phi_{int} = \left(\frac{r_{cl}}{r_p} \right)^{d_f-3} \rightarrow (2)$$

The current work will investigate the aggregate size distribution by studying the volume fraction of alumina nanoparticles in the aggregate cluster (ϕ_{int}) versus cluster size (r_{cl}). The results will be presented as a function of sonication time and overall volume fraction of alumina nanoparticles, ranging from 1% to 5% in the base fluid, at 70 W and 100 W.

7.0 RESULTS: ANALYSIS AND INFERENCE

Figure 5 and Figure 6 shows volume fraction of alumina nanoparticles in the aggregate as a function of cluster diameter, at 70 W, for different sonication times and overall alumina volume fractions respectively. Figure 5 shows that for a specific sonication time, the overall volume fraction of alumina nanoparticles ($\phi_{overall}$) has negligible effect on the number of nanoparticles contained in any given aggregate (ϕ_{int}) at different cluster radii (r_{cl}). It is evident from Figure 5 that increase in sonication time from 20 minutes to 65 minutes, increases the number of particles contained in a given cluster and therefore, the cluster size increases. However, after 80 minutes of sonication, the cluster size is limited to 1000 nm diameter. Based on these results, it can be concluded that the energy gained by the nanofluid through sonication promotes cluster growth and increases the number of particles per cluster. At the same time, beyond 80 minutes, the sonication energy gained breaks larger clusters and limits the cluster size to 1000 nm diameter.

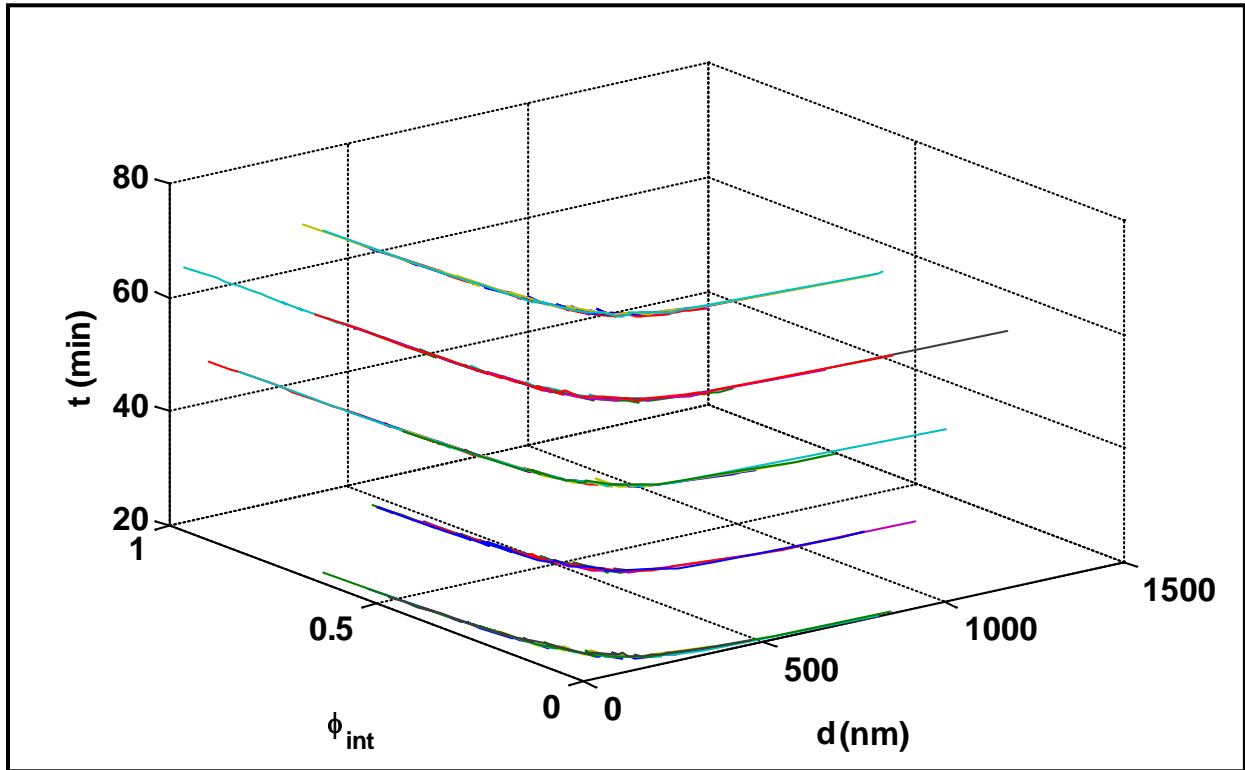


Figure 5. Volume Fraction of Nanoparticles in the Aggregate versus Cluster Diameter as a function of sonication time at 70 W

Similarly, the results contained in Figure 6, indicates that at a given volume fraction of alumina nanoparticles ($\phi_{overall}$), sonication time had negligible effect on the number of nanoparticles contained in any given aggregate (ϕ_{int}) at different cluster radii (r_{cl}).

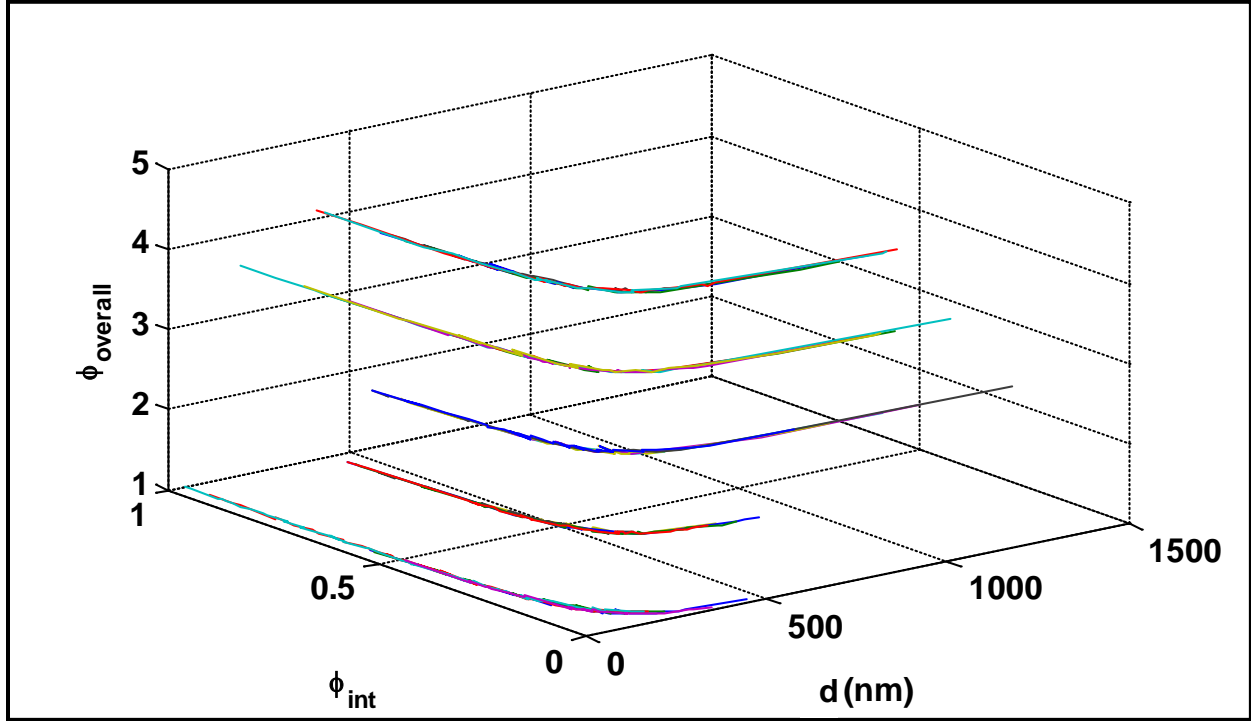


Figure 6. Volume Fraction of Nanoparticles in the Aggregate versus Cluster Diameter as a function of Overall Volume Fraction of Alumina Nanoparticles at 70 W

In Figure 6, when $\phi_{overall}$ is 1%, the nanoparticles were finely dispersed resulting in smaller clusters having the highest number of particles per aggregate with the size of the largest cluster limited to a diameter of 500 nm. As $\phi_{overall}$ increases to 2%, there is a marginal growth in larger clusters and the volume fraction of particles in a single aggregate drops significantly at lower cluster diameter. At $\phi_{overall} = 3\%$, more alumina nanoparticles particles increases cluster size while the number of particles per aggregate remains a constant. When $\phi_{overall}$ increases to 4%, the cluster diameter remains constant while the number of particles per aggregate increases at lower diameter. This means that particles that were added directly dispersed, or resulted in cluster containing only a few particles. This trend holds when $\phi_{overall}$ is at 5% volume fraction. This conclusion holds true for results obtained at 100 W sonication, as shown in Figure 7 and Figure 8.

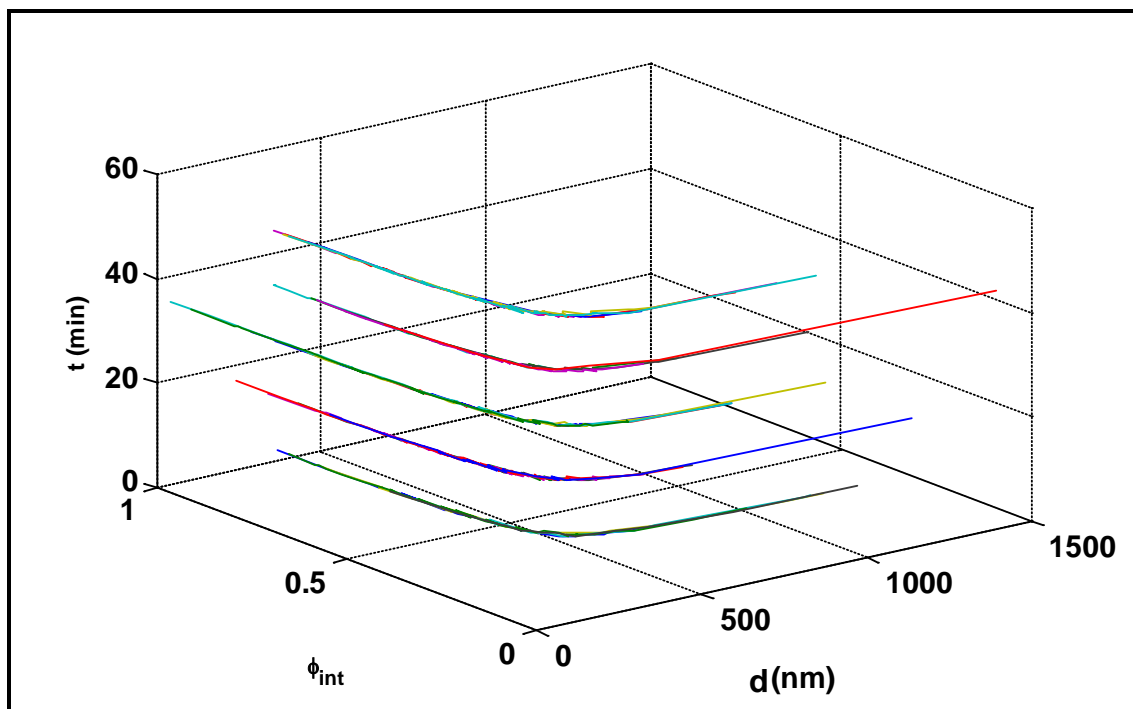


Figure 7. Volume Fraction of Nanoparticles in the Aggregate versus Cluster Diameter as a function of sonication time at 100 W

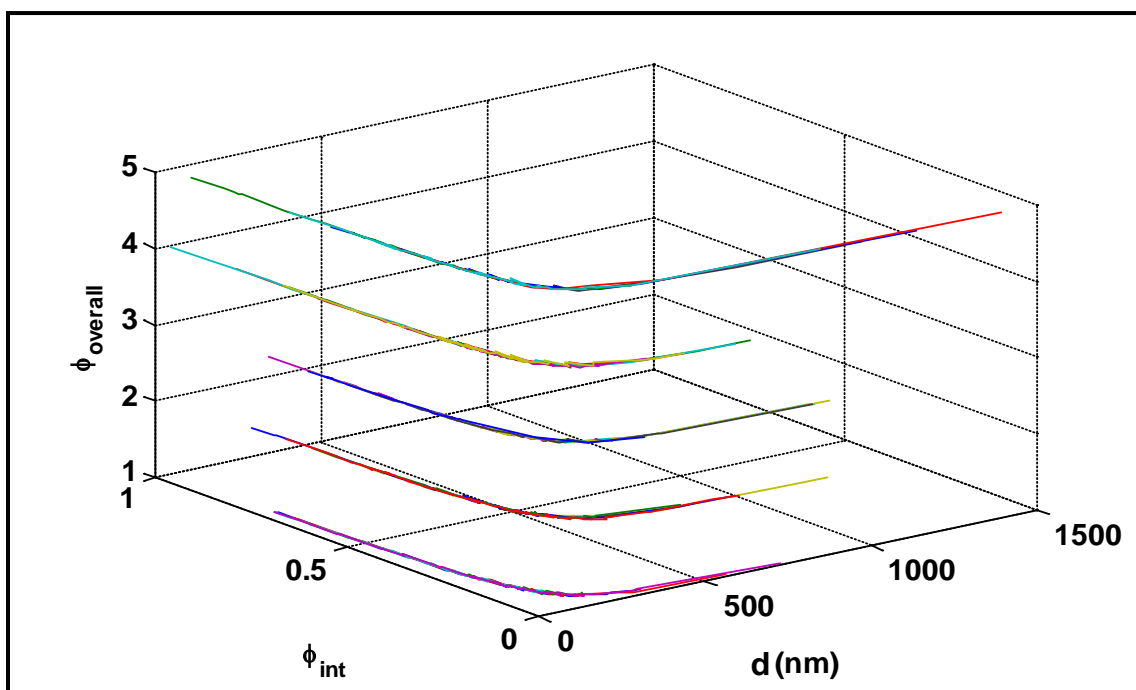


Figure 8. Volume Fraction of Nanoparticles in the Aggregate versus Cluster Diameter as a function of Overall Volume Fraction of Alumina Nanoparticles at 100 W

The important conclusion is that increase in sonication time did not have a significant change in cluster growth and number of particles per aggregate when the overall volume fraction of alumina nanoparticles is a constant.

8.0 CONCLUSIONS AND RECOMMENDATIONS FOR FUTURE WORK

The cluster size distribution and the number of particles per cluster in the alumina nanofluid have been characterized as a function of sonication time and overall nanoparticles volume fraction at two different power levels. It has been concluded that at both power levels, sonication time has negligible effect on the cluster size and the number of particles per cluster when the overall volume fraction is a constant and vice versa. These results have direct implications on the overall thermal conductivity enhancement of the nanofluid. The smaller clusters that contain larger fraction of particles compared to the base fluid tend to have a higher thermal conductivity compared to larger clusters with fewer particles and a large fraction of the base fluid. Therefore, enhancement in thermal conductivity can be maximized by optimizing the size of smaller clusters. Figure 9 substantiates this conclusion and shows the thermal conductivity of clusters at all sonication times and volume fractions at 100 W.

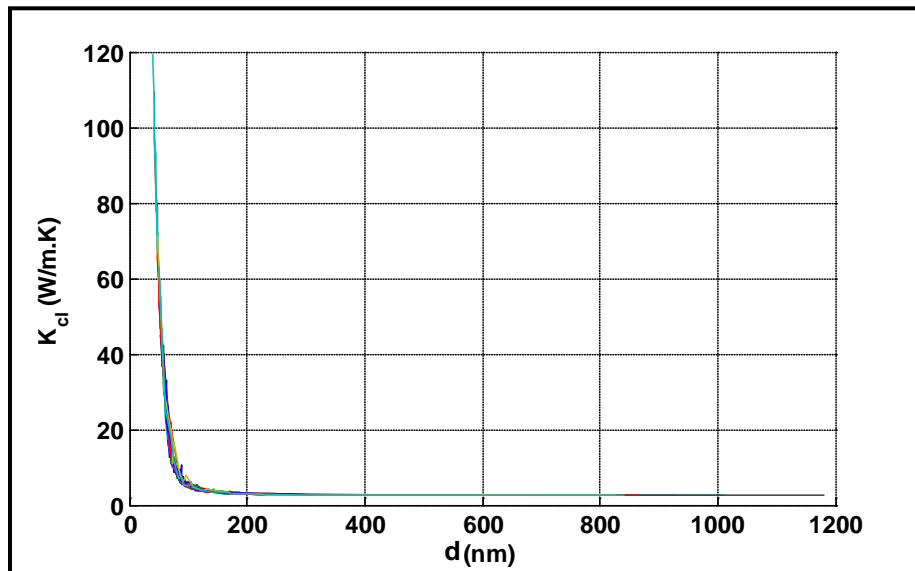


Figure 9. Thermal Conductivity of Clusters at 100 W for all Sonication Times and Overall Volume Fraction of Alumina Nanoparticles

Based on the fact that the fraction of particles in the cluster rapidly decreases with cluster size, it can be concluded that the overall thermal conductivity enhancement can be maximized by limiting the cluster size to a hydraulic mean diameter less than 200 nm. The thermal conductivity of the clusters are marginally higher than the base fluid and is almost a constant beyond 200 nm.

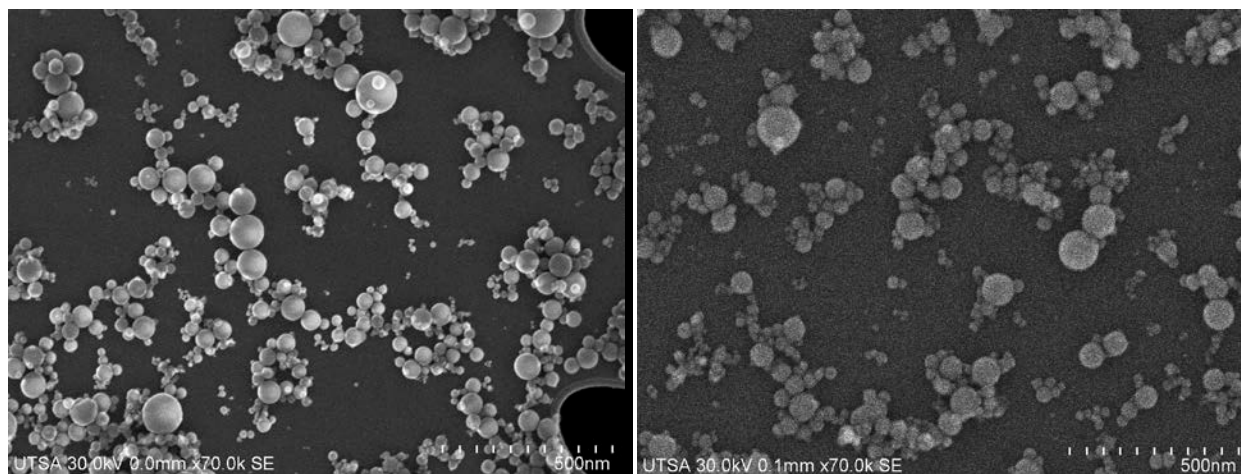
The current research work has established the fact that optimizing the cluster distribution or increasing the volume fraction of particles in cluster cannot be solely achieved by sonication parameters, such as time or power level, while preparing the nanofluid. Rather, particles should be modified prior to dispersion by sonication. An approach to such modification includes encapsulation of nanoparticles using sol-gel process. Future work should emphasize on optimizing and limiting the cluster size to yield a high thermal conductivity nanofluid by modifying nanoparticles prior to dispersion by sonication.

9.0 REFERENCES

- Jeyashekar N, Johnson J. E., Hutzler S. E., Frame E. (2012) *“Modeling the Effect of Agglomeration in Nanoparticle Coolant Systems Using Dynamic Light Scattering.”* Interim Report TFLRF No. 420, ADA572409, January 2012.
- Oxley JD (1998) Environmental Applications of Ultrasound. Doctoral Thesis, University of Illinois at Urbana-Champaign, Champaign, IL, USA.
- Özerinç S, Kakaç S, Yazicioğlu AG (2009) Enhanced thermal conductivity of nanofluids: a state-of-the-art review. *Microfluid Nanofluid* 8:145-190.
- Wang BX, Zhou LP, Peng XF (2003) A fractal model for predicting the effective thermal conductivity of liquid with suspension of nanoparticles. *International Journal of Heat and Mass Transfer* 46:2665-2672.

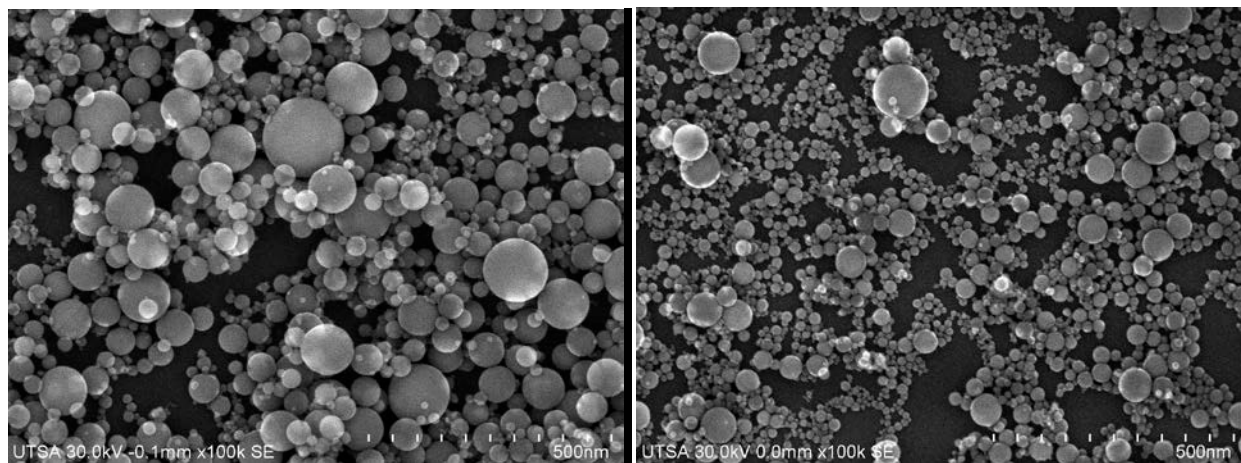
APPENDIX A.
SEM Images of Alumina Nanofluids at Different Sonication times, Volume
Fractions and Sonication Power Levels

UNCLASSIFIED



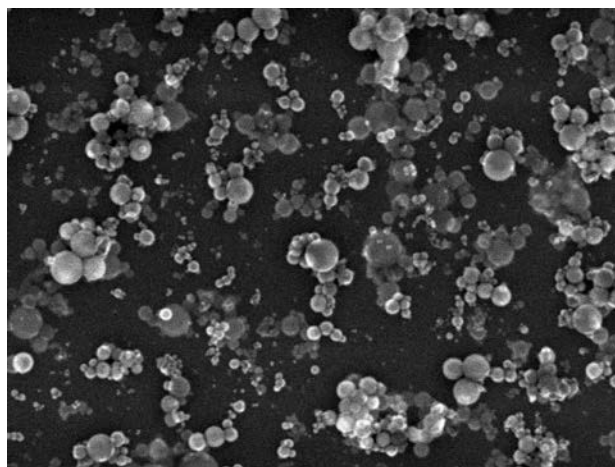
20 minutes

35 minutes



50 minutes

65 minutes

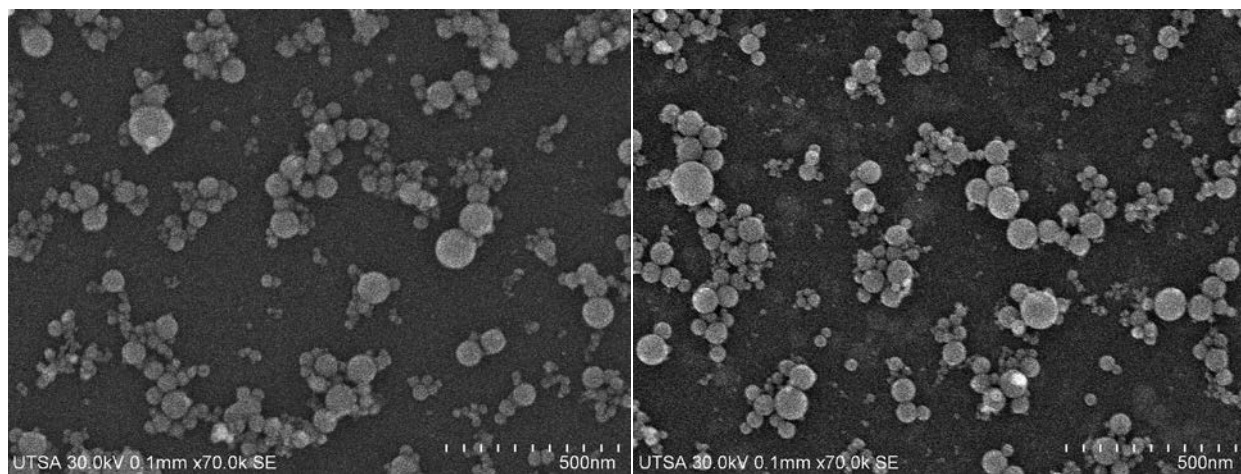


80 minutes

Figure A-1. $\phi_{\text{overall}} = 1\%$, $P = 70 \text{ W}$

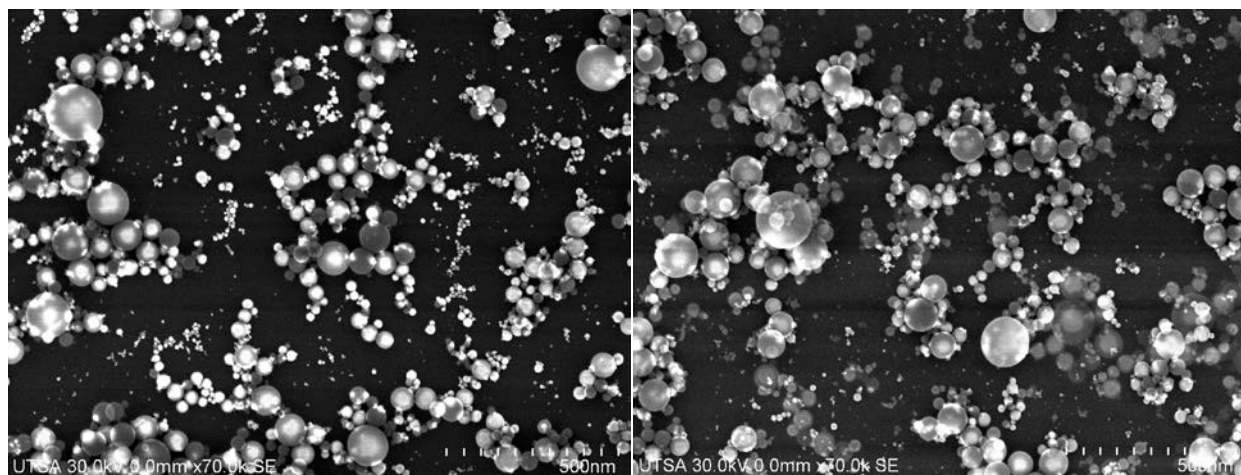
UNCLASSIFIED

UNCLASSIFIED



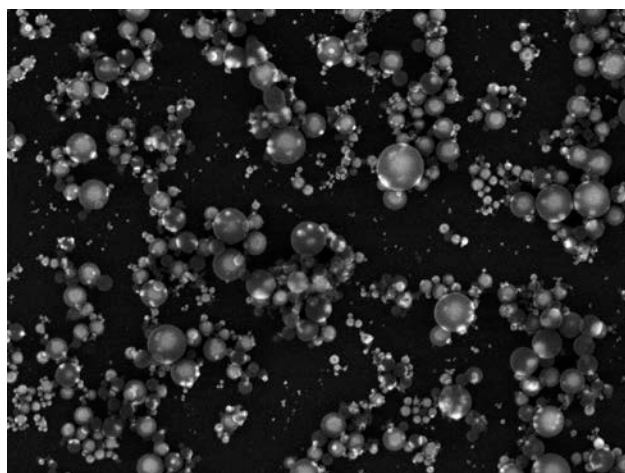
20 minutes

35 minutes



50 minutes

65 minutes



80 minutes

Figure A-2. $\phi_{\text{overall}} = 2\%$, $P = 70 \text{ W}$

UNCLASSIFIED

UNCLASSIFIED

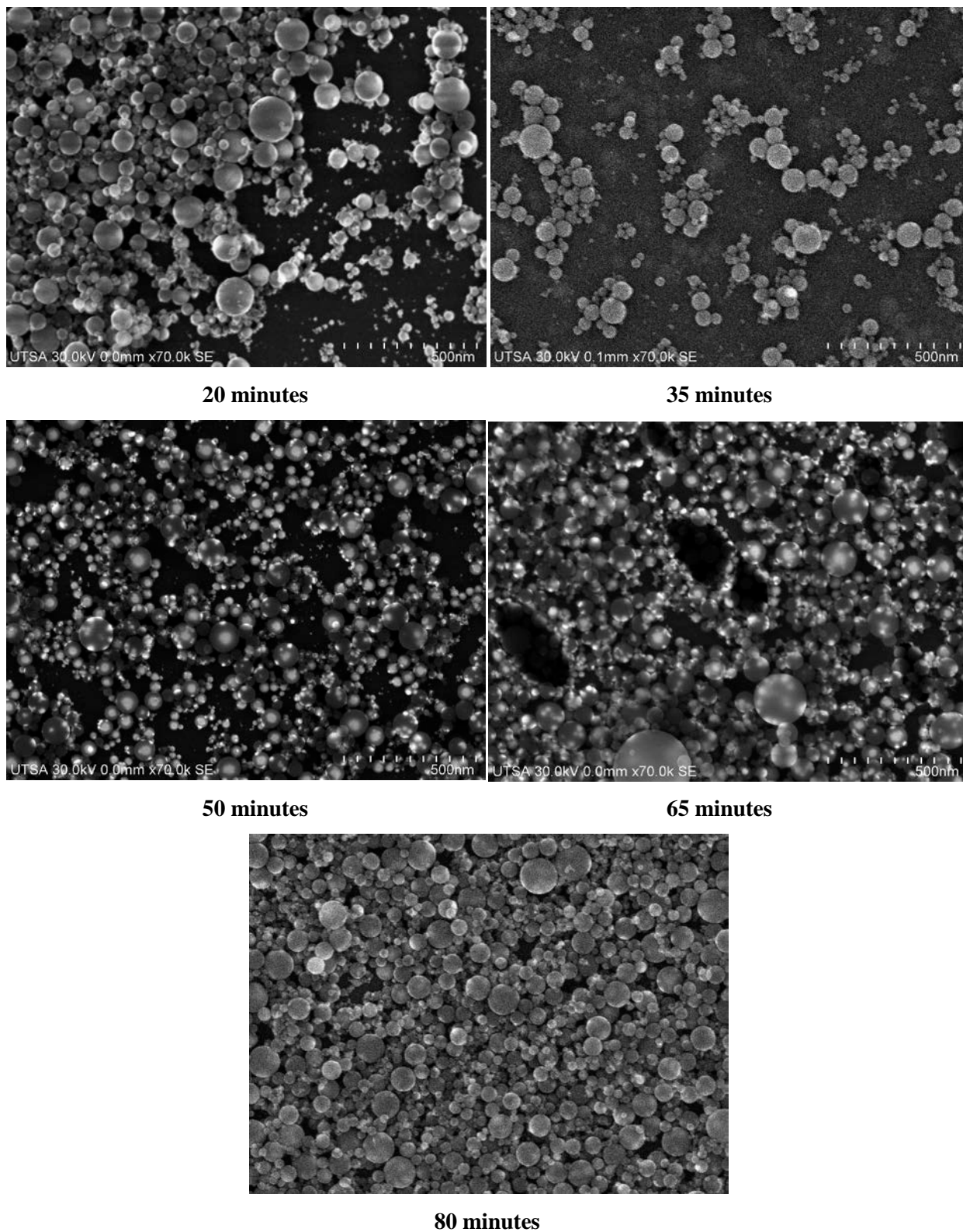
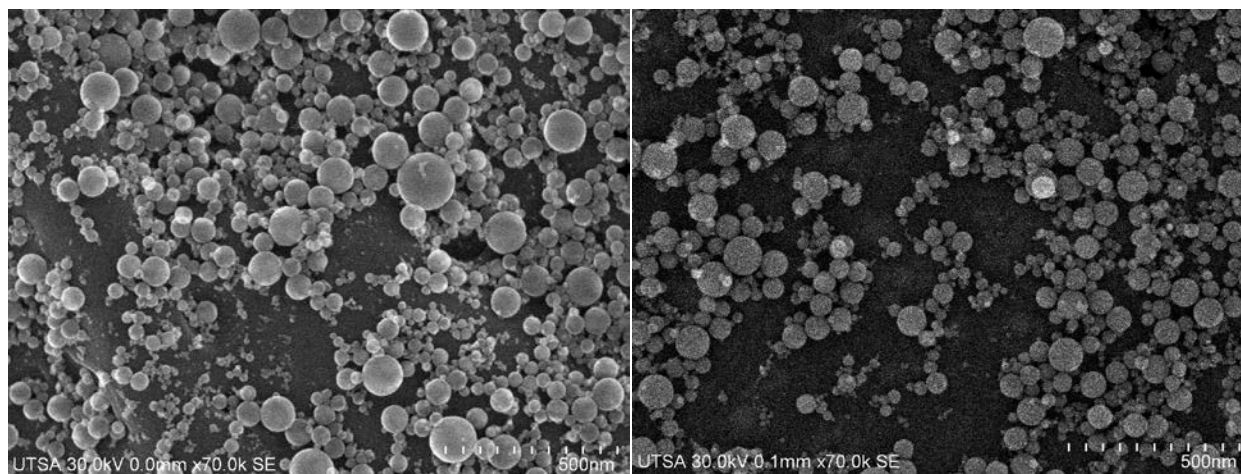


Figure A-3. $\phi_{\text{overall}} = 3\%$, $P = 70 \text{ W}$

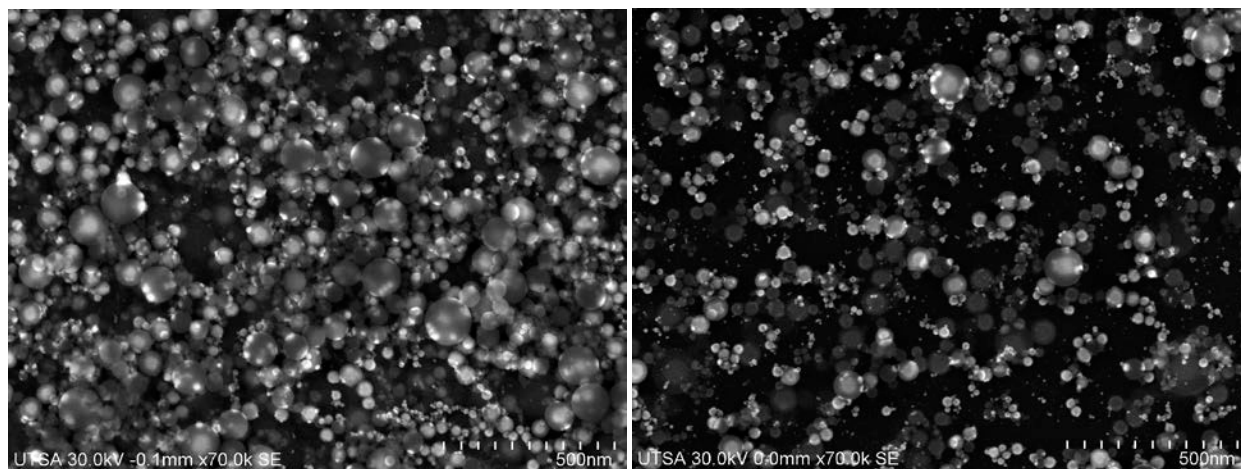
UNCLASSIFIED

UNCLASSIFIED



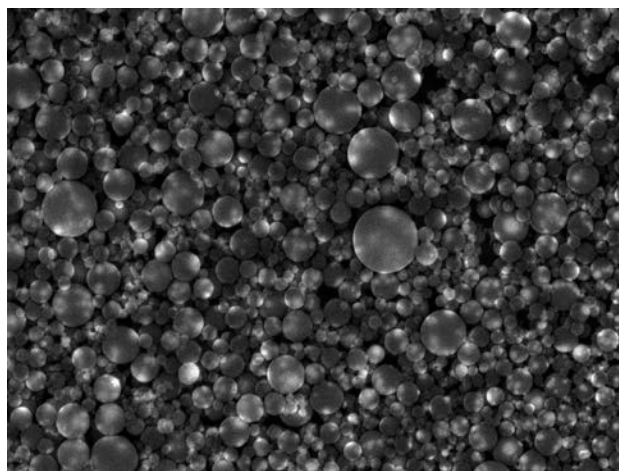
20 minutes

35 minutes



50 minutes

65 minutes

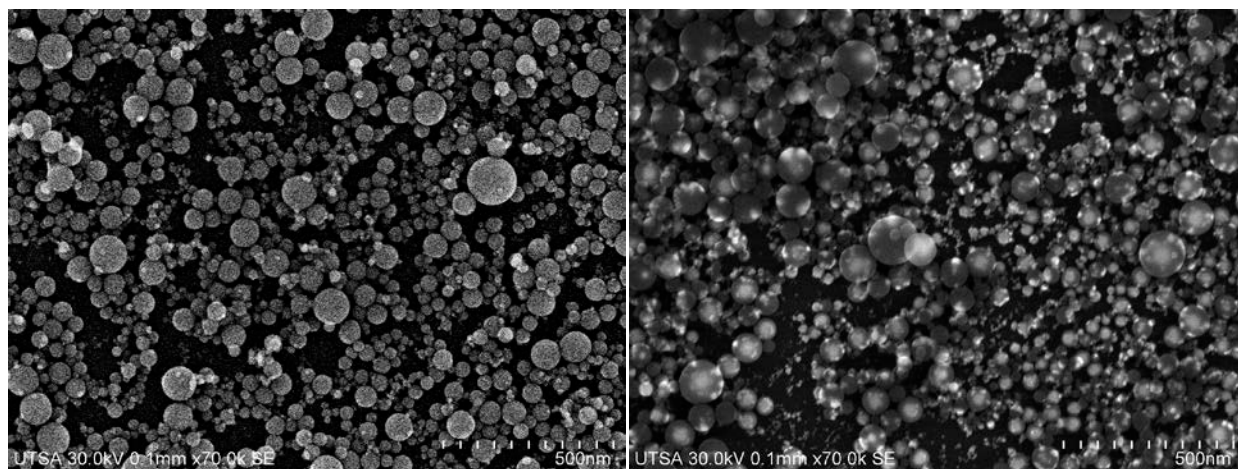


80 minutes

Figure A-4. $\phi_{\text{overall}} = 4\%$, $P = 70 \text{ W}$

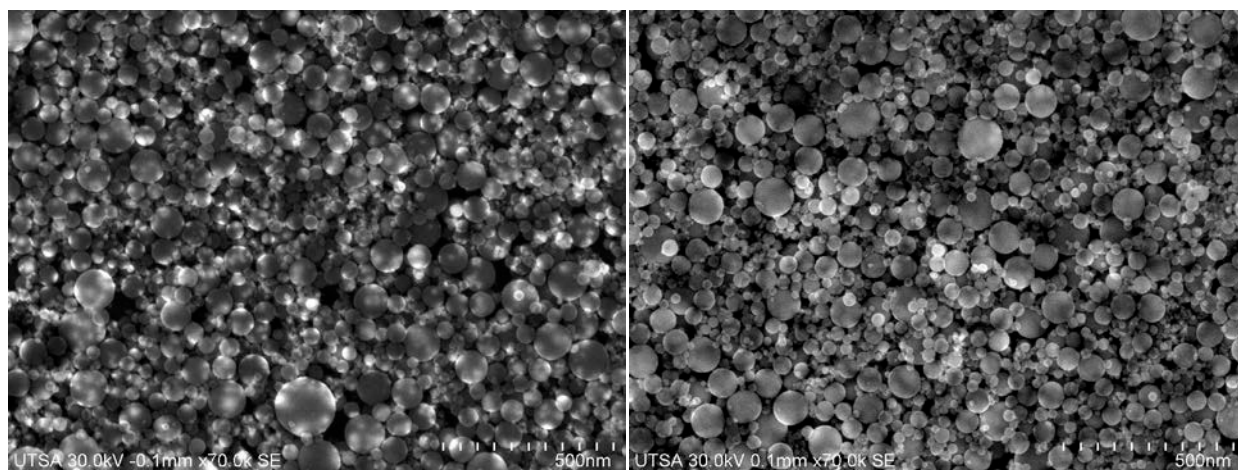
UNCLASSIFIED

UNCLASSIFIED



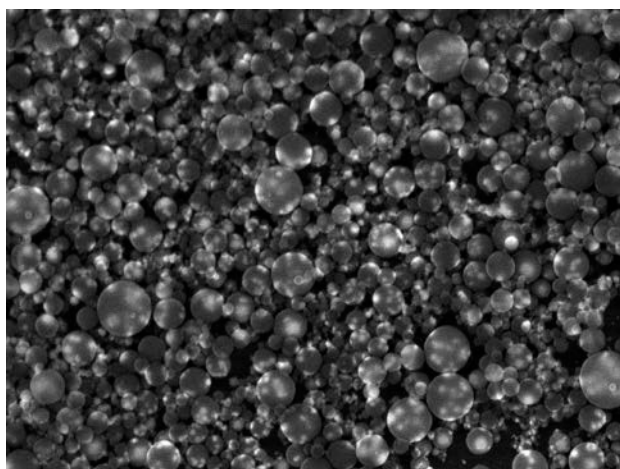
20 minutes

35 minutes



50 minutes

65 minutes



80 minutes

Figure A-5. $\phi_{\text{overall}} = 5\%$, $P = 70 \text{ W}$

UNCLASSIFIED

UNCLASSIFIED

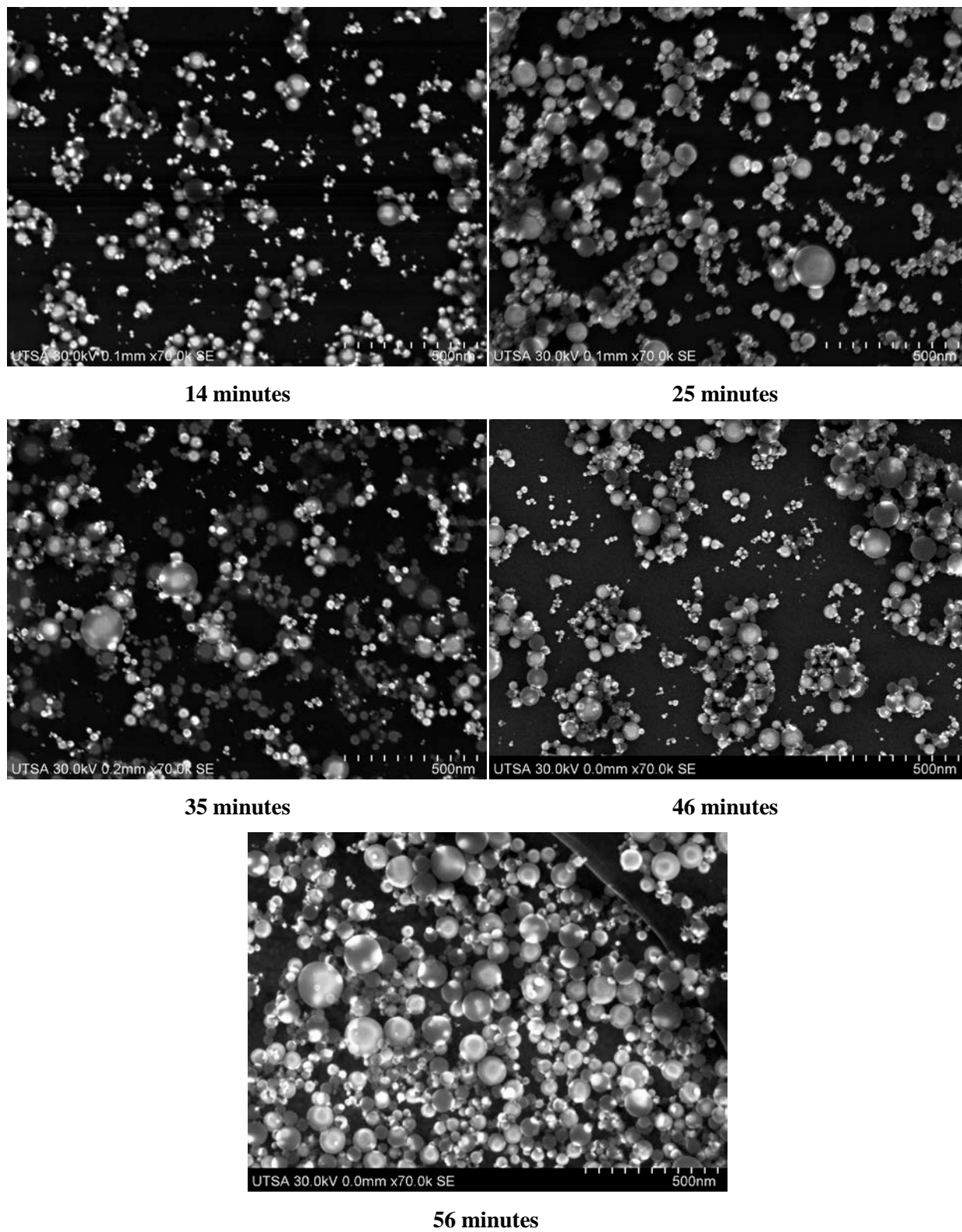
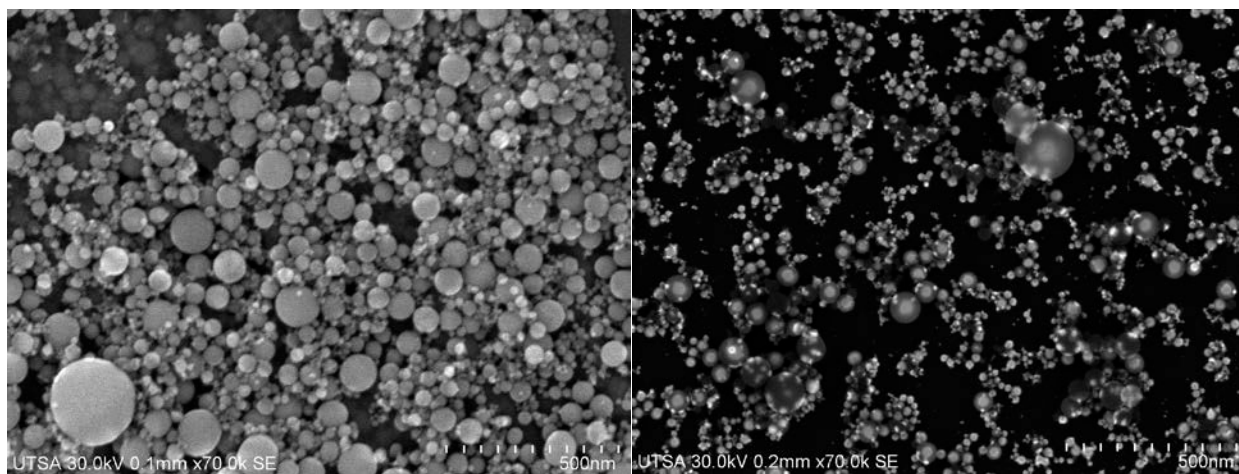


Figure A-6. $\phi_{\text{overall}} = 1\%$, $P = 100 \text{ W}$

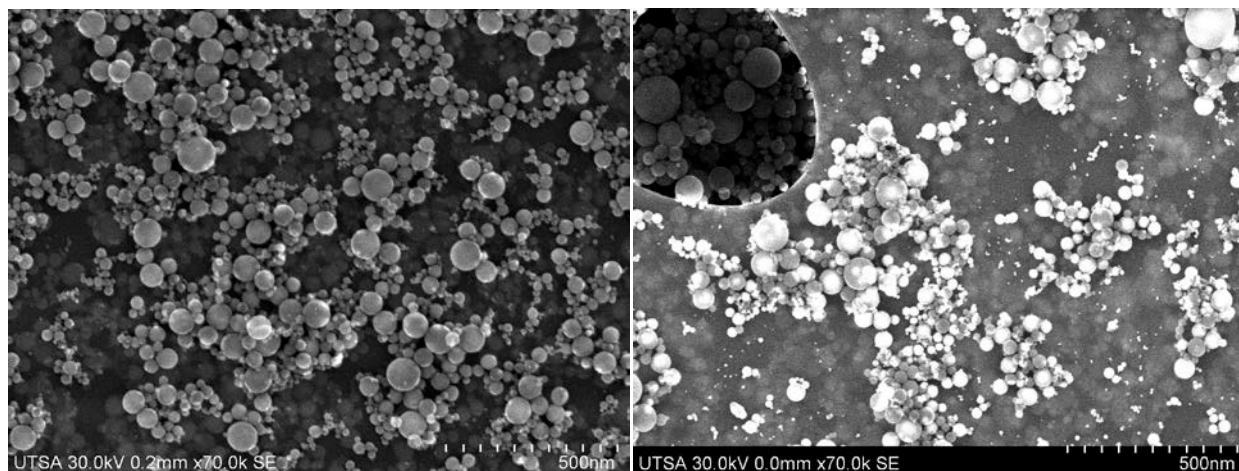
UNCLASSIFIED

UNCLASSIFIED



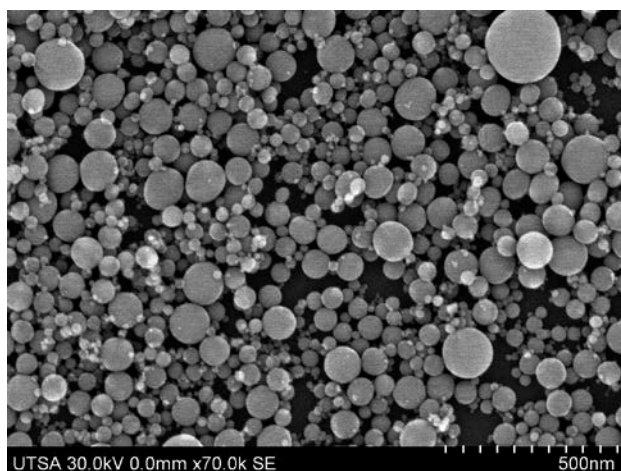
14 minutes

25 minutes



35 minutes

46 minutes



56 minutes

Figure A-7. $\phi_{\text{overall}} = 2\%$, $P = 100 \text{ W}$

UNCLASSIFIED

UNCLASSIFIED

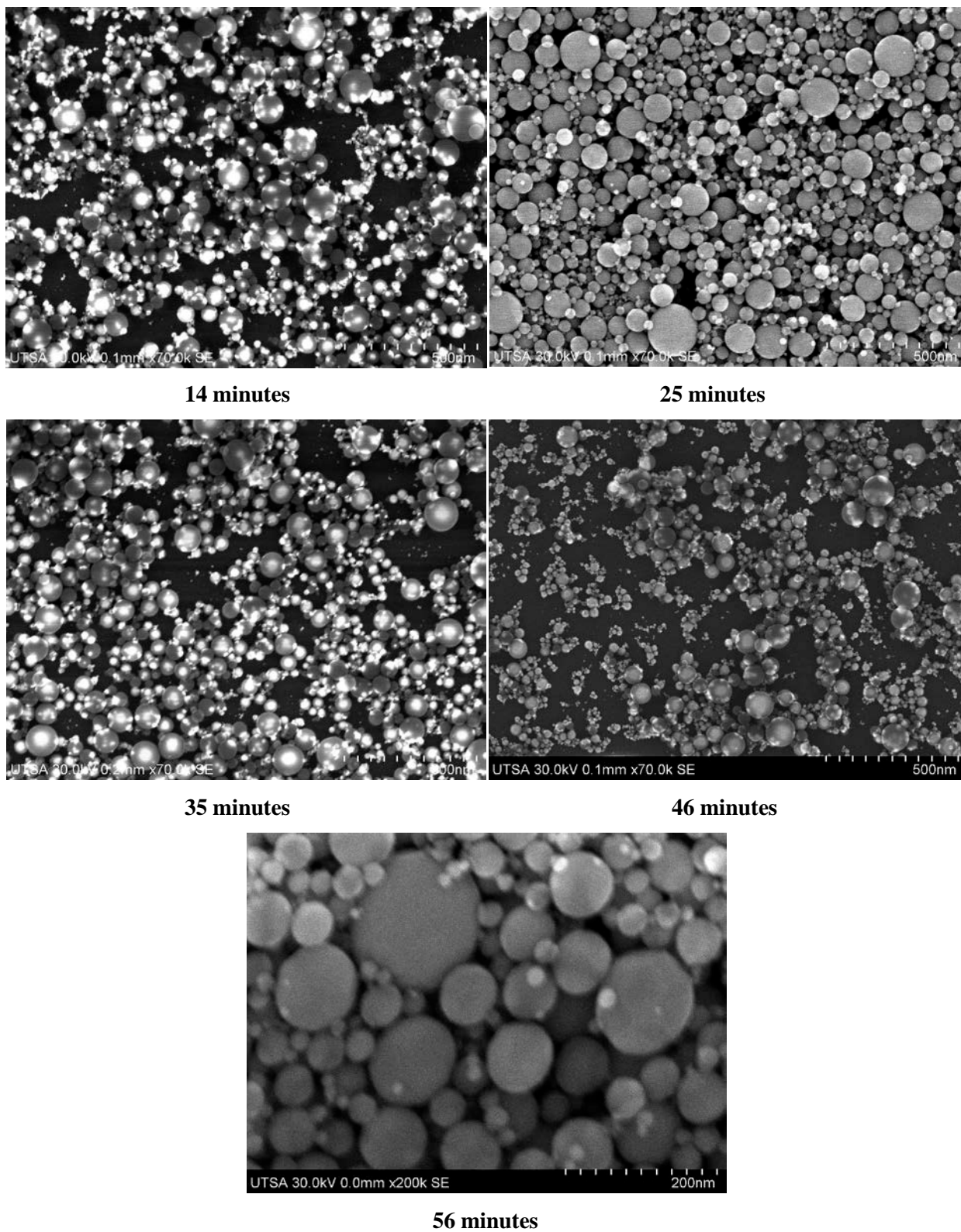
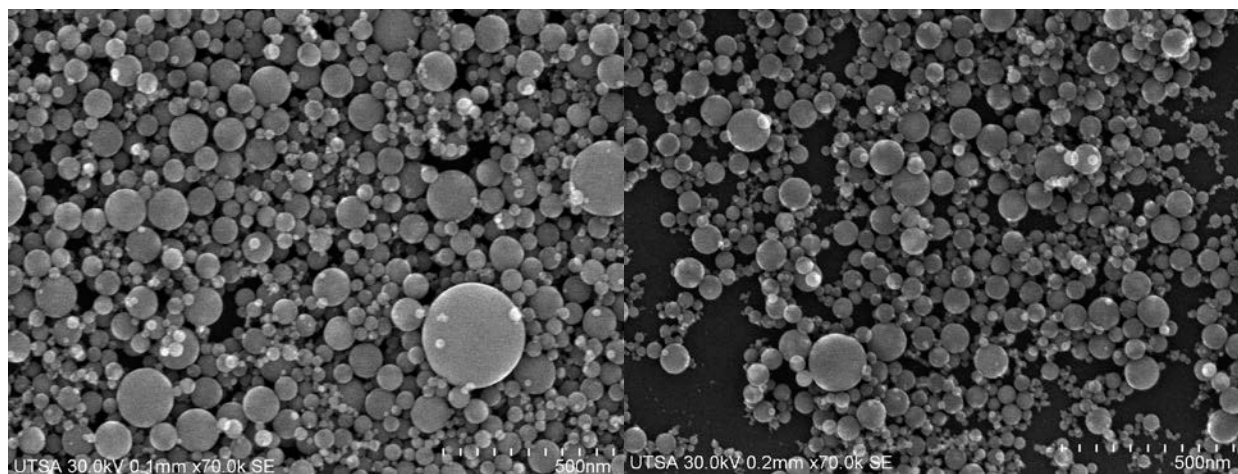


Figure A-8. $\phi_{\text{overall}} = 3\%$, $P = 100 \text{ W}$

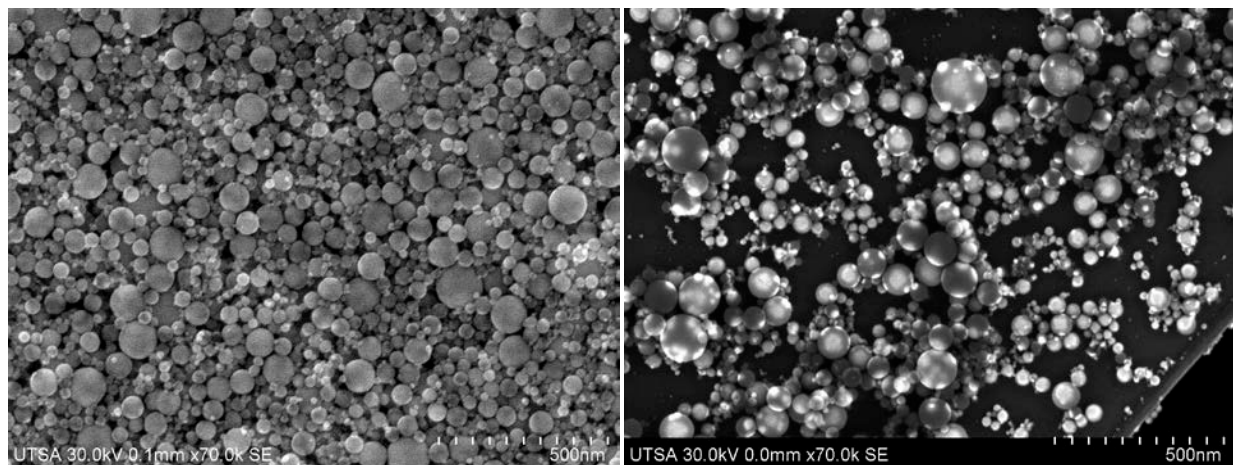
UNCLASSIFIED

UNCLASSIFIED



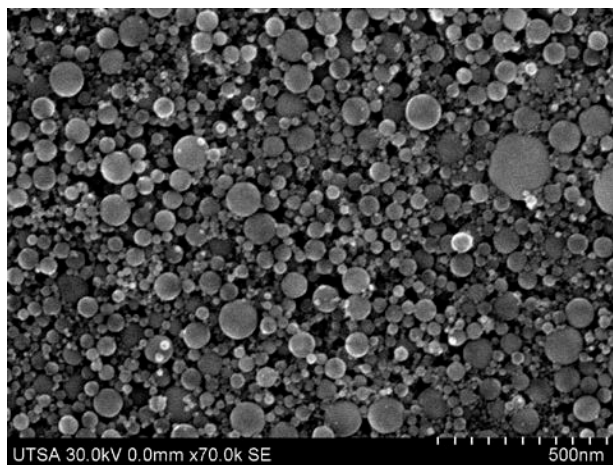
14 minutes

25 minutes



35 minutes

46 minutes

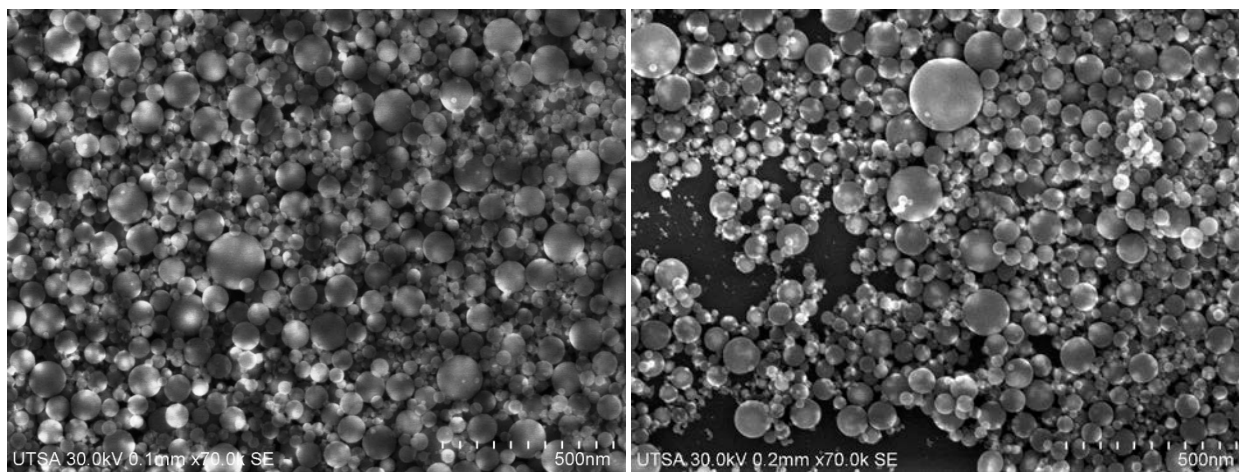


56 minutes

Figure A-9. $\phi_{\text{overall}} = 4\%$, $P = 100 \text{ W}$

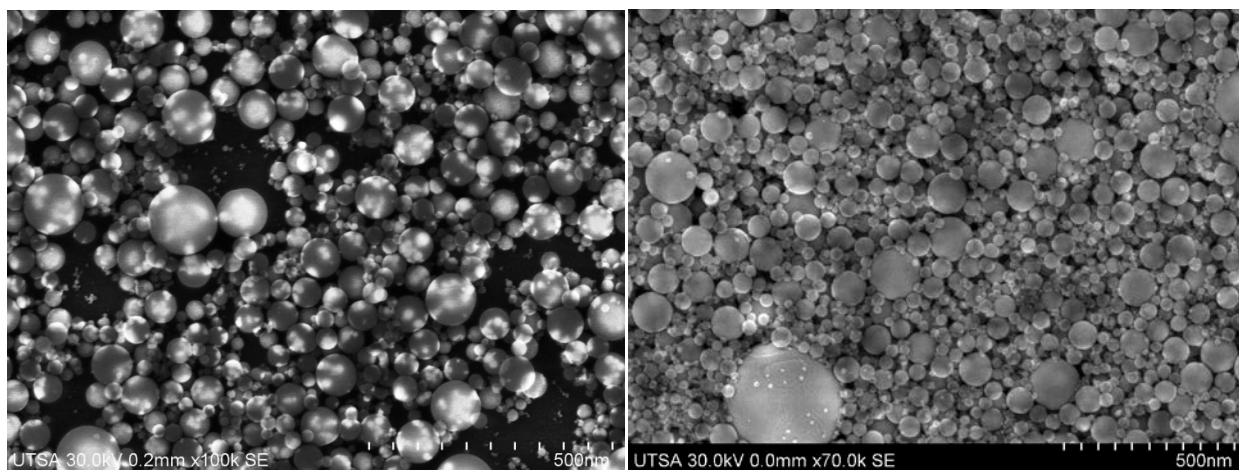
UNCLASSIFIED

UNCLASSIFIED



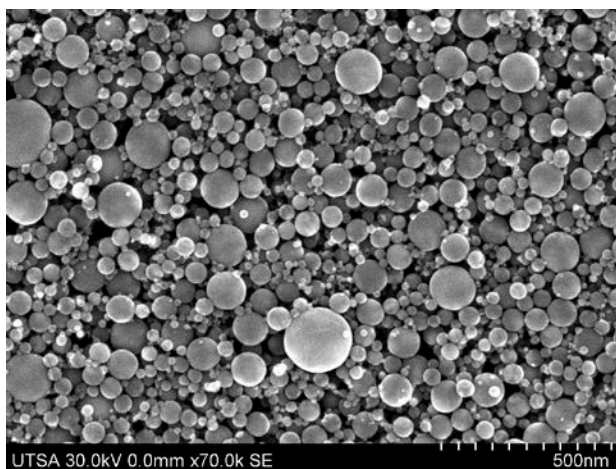
14 minutes

25 minutes



35 minutes

46 minutes



56 minutes

Figure A-10. $\phi_{\text{overall}} = 5\%$, $P = 100 \text{ W}$

UNCLASSIFIED